

Analytical Model of the Coupling Capacitance between Cylindrical Through Silicon Via and Horizontal Interconnect in 3D IC

Wenjian Yu*, Siyu Yang, and Qingqing Zhang

Department of Computer Science and Technology, Tsinghua University, Beijing 100084, China

* Email: yu-wj@tsinghua.edu.cn

Abstract

An accurate yet fast approach is developed to calculate the 2D coupling capacitance between the through silicon via (TSV) and horizontal interconnect wire in 3D IC. We consider the realistic cylinder shape of TSV, and derive the analytical formulas utilizing the idea of field-based analysis. To improve the accuracy, theoretical and numerical results are used to calibrate the formulas. The proposed approach is compared with the commercial field solver Raphael using advanced finite difference method. For the TSV with diameter between $5\mu\text{m}$ and $10\mu\text{m}$ and wire with length within $20\mu\text{m}$, the error of proposed approach is within 8%. While comparing the computational time, the latter is over 5000X faster than the former.

1. Introduction

One of the promising technologies to continue the Moore's law is the 3D integrated circuit (IC). In 3D IC, the through silicon via (TSV) vertically connects the stacked silicon dies. It provides shorter interconnection, enabling higher clock frequency and lower power consumption. 3D IC also facilitates high-density heterogeneous integration, which largely prompts the development of consumer electronics products. Therefore, 3D IC has become the research focus during recent years [1-7].

As a distinctive component in 3D IC, the TSV brings difficulties to electrical modeling and simulation. Modeling the capacitance effect of TSV is a crucial task in physical design [1, 2]. Most existing works have considered the calculation of the coupling capacitance between TSVs [3-6]. However, in the via-last technology of 3D IC, the coupling between TSV and horizontal interconnect wire is also prominent. In [7], an analytical approach is proposed to calculating this kind of capacitance. However, the TSV was assumed to have square cross-section, which is largely deviated from the reality. The approach in [7] is not applicable to the actual cylindrical TSV.

In Fig. 1, the cross section of a 3D IC with the via-last technology is shown. A TSV passes through the whole

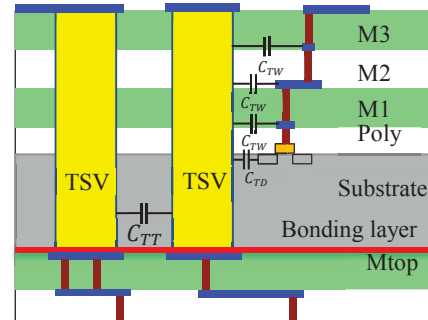


Figure 1. The coupling capacitances of TSV in the via-last technology of 3D IC.

die including the metal layers, which gives rise of different coupling capacitances: C_{TT} (between TSV and TSV), C_{TW} (between TSV and horizontal wire), and C_{TD} (between TSV and device). The calculation of C_{TT} and C_{TD} has been investigated extensively [3-6]. In this letter, we focus on C_{TW} , and develop a fast yet accurate approach for calculating the 2D cross-section capacitance between the cylindrical TSV and horizontal wire. The field-based approach, which was originally used to model the capacitances of rectangular wires [2], is firstly developed for the cylindrical TSV. Then, the calibration techniques are proposed to improve the accuracy. Numerical experiments on the TSV structure with typical parameter settings reveal that the proposed method is over 5000X faster than the Raphael from Synopsys Inc., with at most 8% error.

2. The analytical approach for coupling capacitance between cylindrical TSV and horizontal wire

To calculate the 2D coupling capacitance between cylindrical TSV and horizontal wire, we consider the structure consisting of a circle and a rectangle (see Fig. 2). Below we present the field-based approach and the calibration technique for calculating the capacitance.

2.1 Field-based capacitance modeling

The electrostatic field between the TSV and the wire determines the coupling capacitance. For the structure shown in Fig. 2, we approximately partition the electric field with several regions. Different region of electric field distribution corresponds to different capacitance component. Thus, we have five capacitance components. Because there is little electric field line emitted from

The work is supported in part by National Natural Science Foundation of China (No. 61076034), and Beijing Natural Science Foundation (No. 4132047).

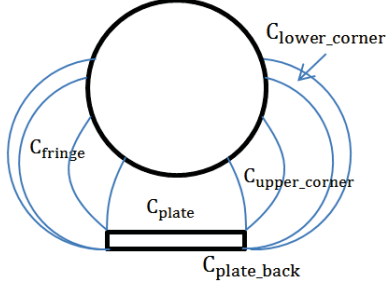


Figure 2. The components of the coupling capacitance of cylindrical TSV.

TSV to the lower corner and the opposite face of the wire, C_{plate_back} and C_{lower_corner} can be ignored. Below, we derive the formulas for C_{plate} , C_{upper_corner} and C_{fringe} respectively.

In electrostatic field, the difference of potential is the integral of electric field:

$$\Delta V = \int_0^D E(l) dl, \quad (1)$$

where $E(l)$ is the electric field intensity and D is the length is electric field line. To calculate C_{plate} , we only consider the field lines between the circle and the top face of rectangle. The end of this line is perpendicular to the top face or the circle. We assume that the value of $E(l)$ varies linearly along the line. So,

$$\Delta V \approx \int_0^D \left(E(0) + \frac{E(D)-E(0)}{D} l \right) dl = \frac{E(0)+E(D)}{2} D, \quad (2)$$

where $E(0)$ and $E(D)$ are the field intensity at the two end points respectively (see Fig. 3). Considering the relationship between conductor surface charge and electric field intensity, we have:

$$E(0)r d\theta = \frac{dQ_c}{\epsilon}, \quad E(D)dx = \frac{-dQ_p}{\epsilon}, \quad (3)$$

where dQ_c and dQ_p stand for the infinitesimal quantity of charge. ϵ is the permittivity of environment. Because the charges connected by a single electric field line has same absolute value, i.e. $dQ_c = -dQ_p$, we derive:

$$\Delta V \approx \frac{D}{2\epsilon} \left(\frac{dQ_c}{rd\theta} - \frac{dQ_p}{dx} \right) = \frac{D \cdot (rd\theta + dx) \cdot dQ_c}{2\epsilon r \cdot d\theta \cdot dx}. \quad (4)$$

With the definition of capacitance,

$$C_{plate} = \frac{Q_c}{\Delta V} \approx \int \frac{2\epsilon}{D(x)} \cdot \frac{rd\theta dx}{rd\theta + dx}, \quad (5)$$

which is an integral on the interval corresponding to the C_{plate} region. And, $D(x)$ denotes the length of electric field line depending on the position of its ending point.

We can assume that the field line between the circle and top surface of wire is an arc [4]. As shown in Fig. 3, we derive the relationship between bias angle θ and the coordinate x of the ending point of electric line:

$$d\theta = \frac{2(d+r)}{(d+r)^2 + x^2} dx, \quad (6)$$

where r is the radius of the circle and d is the distance between the center of circle and the wire. Since

$$D(x) = (x - x_c)\theta, \quad (7)$$

where x_c is the coordinate of the crossing point of the tangent line and the rectangle, we derive with Fig. 3:

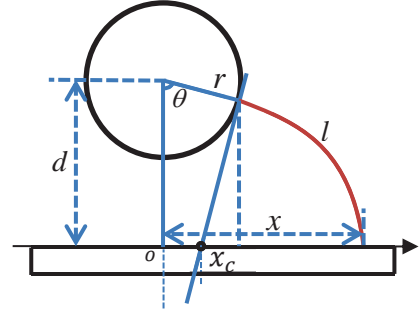


Figure 3. The illustration of electric field line for C_{plate} .

$$x - x_c = \frac{x^2 + d^2 - r^2}{2x}, \quad (8)$$

$$\theta = 2 \tan^{-1} \frac{x}{d+r}. \quad (9)$$

Therefore,

$$D(x) = \frac{x^2 + d^2 - r^2}{x} \cdot \tan^{-1} \frac{x}{d+r}. \quad (10)$$

Substituting (6) and (10) into (5), we get:

$$C_{plate} \approx 2\epsilon \int_0^{\frac{L}{2}} \frac{4xr(d+r)}{(x^2 + d^2 - r^2)[2r(d+r) + (d+r)^2 + x^2] \tan^{-1} \frac{x}{d+r}} dx. \quad (11)$$

This is a formula obtained with the field-based approach, wherein L is the length of wire. To calculate the integral, the numerical quadrature method, like the composite Simpson formulas, can be employed [10].

We now consider the calculation of C_{fringe} . If $L < 2r$, there are some field lines starting from circle to the ends of wire [see Fig. 4(a)]. Otherwise, C_{fringe} is negligible. We also assume that the field line is arc, with radius denoted by R . R, y (which measures the position of field line on the wire width) and θ fulfill the following equations:

$$\begin{cases} r \sin \theta = \frac{L}{2} + R \cos \theta \\ y = R + r \cos \theta + R \sin \theta - d \end{cases}. \quad (12)$$

It derives: $\cos(\frac{\pi-\theta}{2}) / \sin(\frac{\pi-\theta}{2}) = 2(y+d)/(2r-L)$.

So, we have:

$$\theta = \frac{\pi}{2} - 2 \tan^{-1} \left(\frac{2r-L}{2(d+y)} \right), \quad (13)$$

$$R = \frac{2r \sin \theta - L}{2 \cos \theta}. \quad (14)$$

Substituting (13) into (14), we get the length of arc:

$$D(y) = R \left(\frac{\pi}{2} + \theta \right) = \frac{(y+d)^2 - r^2 + (\frac{L}{2})^2}{2(y+d)} \left[\pi - 2 \tan^{-1} \left(\frac{2r-L}{2(d+y)} \right) \right]. \quad (15)$$

Suppose w is the width of the wire. $D(0)$ and $D(w)$ correspond to the shortest and longest electric field lines, respectively. We use their mean value to calculate C_{fringe} :

$$C_{fringe} = 2\epsilon \frac{width}{distance} \approx 2\epsilon \frac{2w}{D(0)+D(w)}. \quad (16)$$

C_{upper_corner} stands for the electric coupling between the vertex B and the circle [see Fig. 4(b)]. Some electric field lines start from point B and end on the circle. We follow the formula in [8]: $C \approx \int r \frac{d\theta}{D}$, where D is the

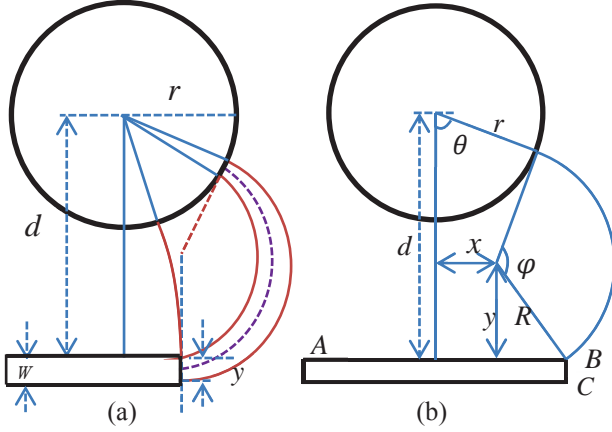


Figure 4. Illustration of calculating (a) C_{fringe} and (b) $C_{upper-corner}$.

length of electric field line, to calculate $C_{upper-corner}$. Assuming the field line is arc, we have the equations:

$$\begin{cases} x = r \sin \theta - R \cos \theta \\ y = d - r \cos \theta - R \sin \theta \\ \left(\frac{L}{2} - x\right)^2 + y^2 = R^2 \end{cases}, \quad (17)$$

where x and y denote the coordinates of the center of arc, and θ is the angle related to the ending point of electric line. Solving (17), we get the formulas for R and φ [see Fig. 4(b)]:

$$R(\theta) = \frac{\left(\frac{L}{2} - r \sin \theta\right)^2 + (d - r \cos \theta)^2}{2 d \sin \theta - L \cos \theta}, \quad (18)$$

$$\varphi(\theta) = 2 \sin^{-1} \frac{\sqrt{\left(\frac{L}{2} - r \sin \theta\right)^2 + (d - r \cos \theta)^2}}{2R}. \quad (19)$$

And, the length of electric line is

$$D(\theta) = R(\theta)\varphi(\theta). \quad (20)$$

The integral interval for calculating $C_{upper-corner}$ depends on two extr eme situations of the electric line. One is the line perpendicular to the top surface of rectangle, and the other is the line perpendicular to the sidewall of rectangle. The value of θ corresponding to the former can be obtained with (9), i.e.:

$$\theta_{min} = 2 \tan^{-1} \frac{L}{2(d+r)}. \quad (21)$$

With Fig. 4(b), we derive the formula for θ_{max} :

$$\theta_{max} = \frac{\pi}{2} - 2 \tan^{-1} \left(\frac{2r-L}{2d}\right). \quad (22)$$

Note that the value of (22) can be larger than π , if $L > 2r$. This should be avoided. So,

$$\theta_{max} = \min\left(\pi, \frac{\pi}{2} - 2 \tan^{-1} \left(\frac{2r-L}{2d}\right)\right). \quad (23)$$

With (18), (19), (21) and (23), we get $C_{upper-corner}$.

$$C_{upper-corner} \approx 2\epsilon \int_{\theta_{min}}^{\theta_{max}} \frac{r}{R(\theta)\varphi(\theta)} d\theta. \quad (24)$$

This integral can be calculated also with the composite Simpson formulas, just like (11).

2.2 Formula calibration

With the field-based approach, (11), (16) and (24) are derived to calculate the three coupling-capacitance components respectively. However, they are based on the

approximations, such as the arc shape of electric field line. Some measures should be adopted to calibrate them to have sufficient accuracy.

Firstly, the formula of C_{plate} can be verified by the situation where the wire is infinitely long. In this case, there is analytical result for the coupling capacitance [9]:

$$C = \epsilon \frac{2\pi}{\ln\left(\frac{d}{r} + \sqrt{\left(\frac{d}{r}\right)^2 - 1}\right)}. \quad (25)$$

Fixing $r=2.5\mu\text{m}$, and setting different values for d , we have calculated C_{plate} with (11) and (25) respectively. The calibration of (11) is shown in Fig. 5.

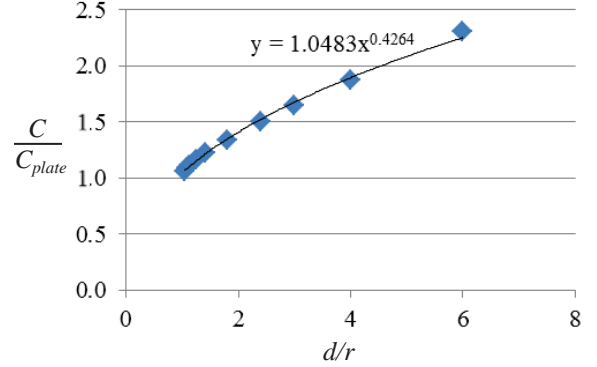


Figure 5. The plot for the ratio of accurate result to C_{plate} , and the calibration formula.

So, the new formula for C_{plate} is:

$$\bar{C}_{plate} = C_{plate} \cdot 1.0483 \left(\frac{d}{r}\right)^{0.4264}, \quad (26)$$

whose maximum error decreases to 2.4%.

For the structure with 80nm-width horizontal wire and $2.5\mu\text{m}$ -radius circle, we set various values of d (up to $10\mu\text{m}$) and various values of L (from $0.2\mu\text{m}$ to $10\mu\text{m}$), and test the accuracy of the field-based approach. The results are compared with Raphael rc2 [11], the golden-value software for capacitance calculation, with a finite difference solver employing advanced nonuniform meshing scheme. The comparison show the maximum discrepancy can be as large as 60%. To alleviate this error, we add a calibration formula to $C_{upper-corner}$, because it is larger than C_{fringe} . With the results from Raphael and the least square fitting technique [10], the new formula for $C_{upper-corner}$ becomes:

$$\bar{C}_{upper-corner} = C_{upper-corner} \cdot [0.0009 \left(\frac{d}{r}\right)^4 - 0.0183 \left(\frac{d}{r}\right)^3 + 0.1321 \left(\frac{d}{r}\right)^2 - 0.1475 \left(\frac{d}{r}\right) + 1.1466], \quad (27)$$

Now, the final formula for calculating the 2D coupling capacitance between cylindrical TSV and horizontal wire becomes:

$$C_{2D} = \bar{C}_{plate} + C_{fringe} + \bar{C}_{upper-corner}. \quad (28)$$

Multiplying it with the height of wire, we can estimate the coupling capacitance.

3. Numerical results and conclusions

More experiments with different values of r (radius of circle) and w (width of horizontal wire) are carried out. For each configuration, the value of L (length of wire) ranges from a small value to 4 or more times of r . And, several values of d (distance between circle center and wire) are set in the experiments. Detailed settings are listed in Table 1. The wire widths we have tested are the typical settings under the 45nm process technology. And, the radius of TSV conforms to the current manufacturing level. The values of L and d are set such that the structure is of most interest for calculating the coupling capacitance. Also note that, due to the thermal-mechanical stress caused by TSVs, there needs to be a keep-out zone around a TSV [12]. As a result, d should be larger than r to certain extent.

Table 1. Parameter Settings for the Structure with a Cylindrical TSV and a Horizontal Wire

	Other parameters (in unit μm)
$r=2.5\mu\text{m}, w=80\text{nm}$	$L \in [0.2, 10]; d \in [3.5, 7.5]$
$r=5\mu\text{m}, w=80\text{nm}$	$L \in [0.5, 20]; d \in [7, 10]$
$r=2.5\mu\text{m}, w=120\text{nm}$	$L \in [0.2, 10]; d \in [3.5, 7.5]$
$r=5\mu\text{m}, w=120\text{nm}$	$L \in [0.5, 20]; d \in [7, 20]$

For the test structures, the proposed analytical method and Raphael rc2 are used to calculate the capacitance. In Fig. 6, the comparison of the proposed method and Raphael is shown for the structures with $w=80\text{nm}$. The maximum discrepancy between the both methods is 7.3%. For structures with $w=120\text{nm}$, the capacitances are shown in Fig. 7. The maximum error of our method is 8.0%.

All experiments are carried out on a Linux server with Intel Xeon E5506 CPU at 2.13 GHz. Raphael costs about 0.89 second for calculating one structure, while the time of our method is only 0.176 millisecond, on average. This means the proposed method is over 5000X faster than the advanced numerical method.

The major formulas in the proposed approach are (11),

(16), (24), and (26)-(28). They are all functions of d/r , L/r and w/r . So, the proposed model is scalable for different sizes of future TSV and wire. The proposed model is especially suitable for evaluating the signal integrity of TSV during the design of 3D IC. Although we only consider the situation where the wire is aligned in center to the TSV, the approach is also capable of the structure with unaligned wire. In the future, we will further investigate the analytical modeling of all capacitance components for the cylindrical TSV.

References

- [1] M. Grange, R. Weerasekera, D. Pamunuwa, and H. Tenhunen, Design Automation and Test in Europe Conference (2009).
- [2] K. Salah, A. El Rouby, H. Ragai, K. Amin and Y. Ismail, International Symposium on Circuits and Systems, p.2321 (2011)
- [3] I. Savidis and E. G. Friedman, IEEE Trans. ED, 56, p.1873 (2009).
- [4] C. Liu, T. Song, J. Cho, J. Kim, J. Kim and S. K. Lim, Design Automation Conference, p.783 (2011).
- [5] C. Xu, H. Li, R. Suaya, and K. Banerjee, IEEE Trans. ED, 57, p.3405 (2010).
- [6] G. Katti, M. Stucchi, K. De Meyer, W. Dehaene, IEEE Trans. ED, 57, p.256 (2010).
- [7] D. H. Kim, S. Mukhopadhyay and S. K. Lim, IEEE Trans. CPMT, 1, p.168 (2011).
- [8] W. Zhao, X. Li, S. Gu, S. H. Kang, M. M. Nowak and Y. Cao, IEEE Trans. ED, 56, p.1862 (2009).
- [9] C. P. Yuan and T. N. Trick, IEEE Electron Device Letters, 3, p.391 (1982).
- [10] W. Yu, *Numerical Analysis and Algorithms*, Tsinghua University Press (in Chinese) (2012).
- [11] Synopsys Inc., *Raphael: 2D, 3D resistance, capacitance and inductance extraction tool*. <http://www.synopsys.com/Tools/TCAD>.
- [12] W.-K. Mak and C. Chu, IEEE Trans. VLSI, 20, p.2345 (2012).

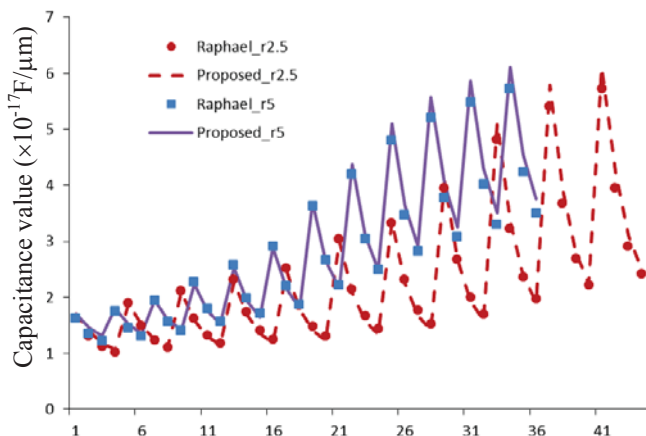


Figure 6. The capacitances obtained with the proposed method and Raphael (width of horizontal wire is 80nm).

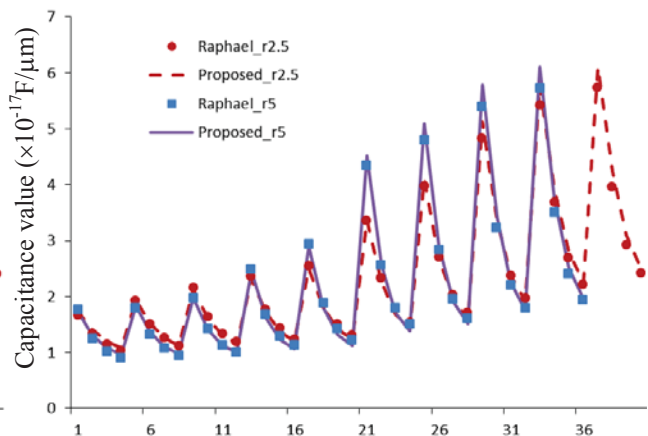


Figure 7. The capacitances obtained with the proposed method and Raphael (width of horizontal wire is 120nm).